Dieses Dokument ist eine Zweitveröffentlichung (Verlagsversion) /

This is a self-archiving document (published version):

Albrecht Hänel, Uwe Teicher, Holger Pätzold, Andreas Nestler, Alexander Brosius

Investigation of a carbon fibrereinforced plastic grinding wheel for high-speed plunge-cut centerless grinding application

Diese Version ist verfügbar / This version is available on:

https://nbn-resolving.org/urn:nbn:de:bsz:14-qucosa2-353796

SLUB
Wir führen Wissen.

TECHNISCHE UNIVERSITÄT DRESDEN

Qucosa
Quality Content of Saxony

Case Study

Investigation of a carbon fibre-reinforced plastic grinding wheel for high-speed plunge-cut centreless grinding application

Albrecht Hänel[1], Uwe Teicher[1], Holger Pätzold[2], Andreas Nestler[1] and Alexander Brosius[1]

Abstract

High-speed plunge-cut centreless grinding opens up enormous potential for the manufacturing of difficult-to-machine materials and to improve the surface quality while reducing the grinding forces. For this investigation, a new grinding wheel base body of carbon fibre-reinforced plastic (CFRP) was developed to achieve grinding wheel speeds up to 150 m/s in plunge-cut centreless grinding of hardened shafts. For evaluation of the performance characteristics, the grinding forces and the surface quality of different grinding tools were detected. These experiments were conducted using a newly developed measuring system to analyse the grinding forces in the workrest blade. The experimental results are described and discussed in this article.

Introduction

Every continuous development in machining production coupled with the development of advanced materials calls for a shift in the technological process limits with regard to grinding,[1] causing new challenges for tool machines and tools.[2] In finishing operations, the high requirements concerning quality also have to be observed, causing minimal technological changes to have a profound impact on the work result.[3]

By increasing the grinding wheel speed in the process with geometrically undefined cutting edges, process limits can be extended, as in processes with geometrically defined cutting edges in the context of high-speed cutting (HSC) machining. A major advantage is the reduction of the load on the abrasive grain and an improvement in the surface quality.[3] In contrast, the increased centrifugal forces produce unpredictable property changes in the grinding wheel, which may have a characteristic negative effect on the work result.[4] In addition, due to the disproportionate relationship between spindle speed and spindle power, significant technological and design expenses are to be expected. For these reasons, research was conducted to analyse

the impact of influence parameters on process stability[5] and process characteristics.[6] One of the main issues for the application of high spindle speeds in centreless grinding is the control of the process stability by adjusting the speed of the workpiece.[7]

Economic relevance is gained through the use of high cutting speeds, especially in the production of mass parts, by extending the current process limitations of the grinding wheel speed during plunge-cut centreless grinding up to $v_s = 150$ m/s. Due to this practice, grinding wheel base bodies made of carbon fibre–reinforced plastic (CFRP) can be used.[8]

For the evaluation of the performance potential of a grinding wheel with a CFRP base body in the process

[1]Institute of Manufacturing Technology, Technische Universität Dresden, Dresden, Germany
[2]Schaeffler Technologies AG & Co. KG, Herzogenaurach, Germany

Corresponding author:
Albrecht Hänel, Institute of Manufacturing Technology, Technische Universität Dresden, 01062 Dresden, Germany.
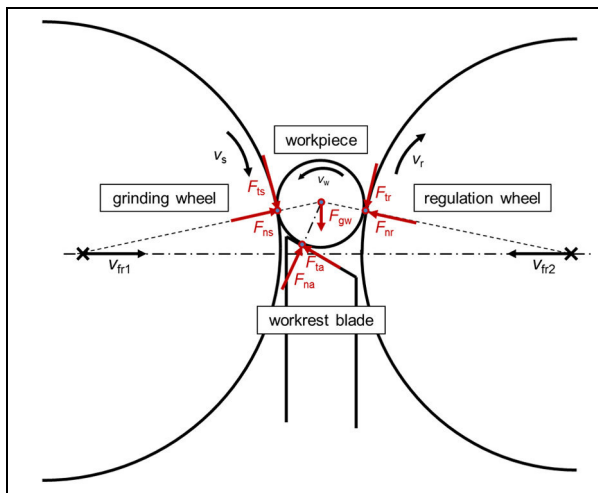Email: albrecht.haenel@tu-dresden.de

Figure 1. Force vectors and moments in the grinding gap.

Figure 2. Force vectores at the work rest blade.

of plunge-cut centreless grinding, the process forces and surface quality on a reference workpiece were analysed.

Experimental conditions

For the investigation of plunge-cut centreless grinding, an analysis and description of the occurring process forces is necessary. The workpiece is cut free to illustrate the force components (Figure 1), which are relevant for the investigation. The reaction forces are being determined accordingly, which can be classified into tangential and normal force components.[9]

Figure 2 shows the equilibrium of forces in the workrest blade and the geometric relationships. This shows that by means of the workrest blade angle β and the measured vertical force F_{yA}, the calculation of the resulting force F_A is possible.[10] This is necessary to comprehend the impact on the grinding process of the workrest blade angle β

$$F_{xA} = F_{tA} \cdot \cos \beta - F_{nA} \cdot \sin \beta \qquad (1)$$

$$F_{yA} = -F_{tA} \cdot \sin \beta - F_{nA} \cdot \cos \beta \qquad (2)$$

As part of the experimental investigations, the tangential force (F_{tS}) was determined. Furthermore, the vertical force (F_{yA}) was measured by means of a specially designed workrest blade (Figure 3). For this purpose, a divided workrest blade was constructed, in which two piezoelectric force sensors from the company Kistler (9132A slimline sensor) were installed. The integration of a triaxial force sensor was not possible due to the low grinding gap of 12 mm. The experimental setup is shown in Figure 4.

The sensors are integrated 20 mm below the contact surface of the workrest blade (Figure 3). This was done, on one hand, in order to minimise the error which may occur through the bending of the upper section and, on the other hand, to ensure the necessary stability in the grinding gap.[11] The sampling rate was set to 2000 Hz.
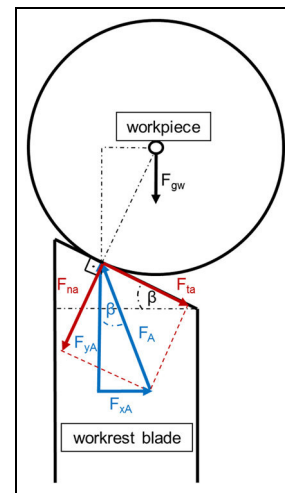
To determine the tangential force F_{tS}, the total power P_t of the grinding spindle was recorded. The average power P_c can be determined by subtracting the idle load power P_l. By means of the grinding wheel speed v_s, the tangential force F_{tS} is calculated

$$P_c = P_t - P_l \qquad (3)$$

$$F_{tS} = \frac{P_c}{v_s} \qquad (4)$$

Experimental procedure

During plunge-cut centreless grinding, the grinding process is divided into several stages: rough machining, semi-finishing, fine finishing and sparking-out (Figure 5). This is achieved by changing the radial displacement in the direction of the radial feed speed $v_{fr_{1,2}}$, whereby different material removal rates are achieved. The required quality in terms of surface roughness is generated in the fine finishing and sparking-out phases, which are characterised by very low material removal rates.[12] Each individual test was repeated five times. Relevant information of the workpiece can be found in Table 1.

As testing machine, a MIKROSA KRONOS S 250 (Figure 6) with a maximum spindle power of 15 kW was selected. Due to the use of a hybrid bearing system of the grinding spindle, a grinding wheel speed up to $v_s = 150$ m/s can be achieved.

Grinding tools

Two different modifications of the grinding tools were applied, which were utilised up to their maximum allowable speed. More relevant information can be found in Table 2.

The segmented grinding wheel (Figure 7) has been newly developed for this investigation and is used up to a grinding wheel speed of $v_s = 150$ m/s. The grinding wheel base body is a hybrid construction and made of CFRP and an inner ring of C45 steel (1.0503). The
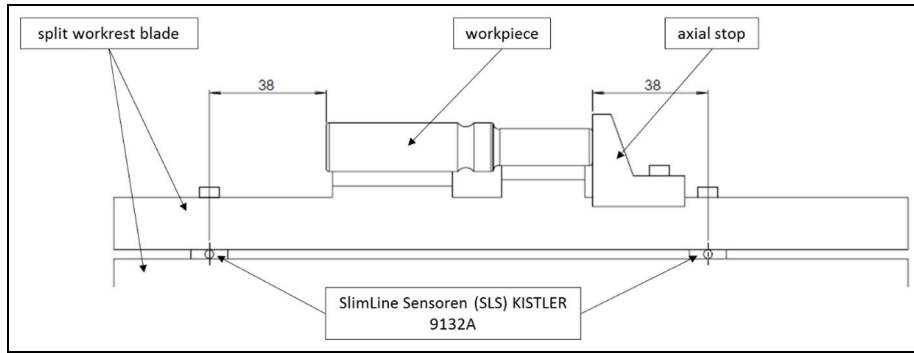
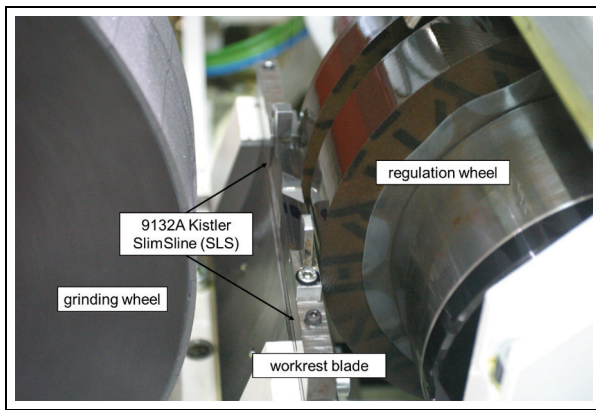**Figure 3.** Schematic layout of the workrest blade with integrated force sensors.

Figure 4. Workrest blade with integrated force sensors, grinding wheel and regulation wheel.
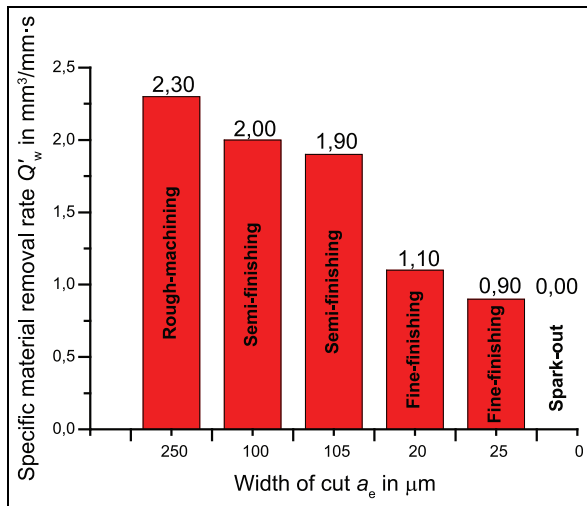

Figure 6. Test machine MIKROSA KRONOS S 250.

Figure 5. Multilevel process management.

Table 1. Experimental parameters.

Grinding process	Plunge-cut centreless grinding
Grinding wheel speed	$v_s = 50$–$150\,m/s$
Cooling	Grinding oil Wiolan SH8.3 (0.3 MPa)
Workpiece	Shaft, hardened
	1.3305 (100Cr6) with $62 \pm 2\,HRC$,
	depth of hardening: 2 mm
Regulation wheel	Diameter: 250 mm, width: 80 mm
Workrest blade angle	30°

grinding wheel can optimally be mounted on the spindle and a high degree of concentricity can be ensured. The grinding wheel base body is a wound body in which the fibres are deposited circumferentially. The grinding wheel has a weight of 21.85 kg. This corresponds to approximately one-quarter of the weight of a grinding wheel base body made of steel. The choice of grain size and concentration was based on a predetermined average surface roughness (axial on the outer surface with $R_z < 3\,\mu m$ and $R_a < 0.5\,\mu m$); thereby, a comparison of the different grinding wheel specification was possible.

Results and discussion

Maximum tangential force F_{tsmax} on the grinding wheel

Figure 8 shows the maximum tangential force F_{tsmax} for the tested grinding tools, whereby the magnitudes of

Table 2. Modification of the tested tools.

	Modification 1: CRFP-CBN	Modification 2: CFRP-WFA
Grain:	cubic boron nitride (CBN)	white fused alumina (WFA)
Grain size:	B 107	F 80 (FEPA size)
Concentration:	125 Kt/cm^3	–
Bond Type:	vitrified	vitrified
Grinding wheel diameter:	Ø450 mm	Ø450 mm
Grinding wheel body:	CFRP	CFRP
Properties:	Wound body, T-700 fibre, fibre volume content 50%	Wound body, T-700 fibre, fibre volume content 50%

FEPA: Federation of European Producers of Abrasives.
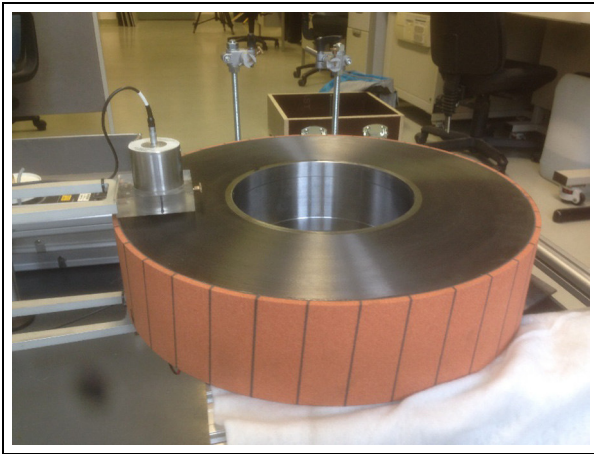
Figure 7. Grinding wheel with CFRP body (Modification 2, CFRP-WFA).

Figure 8. Maximum tangential force F_{tsmax} as a function of the grinding wheel speed v_s.
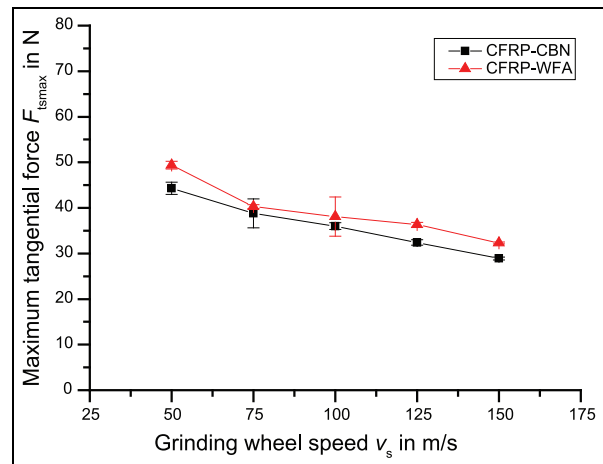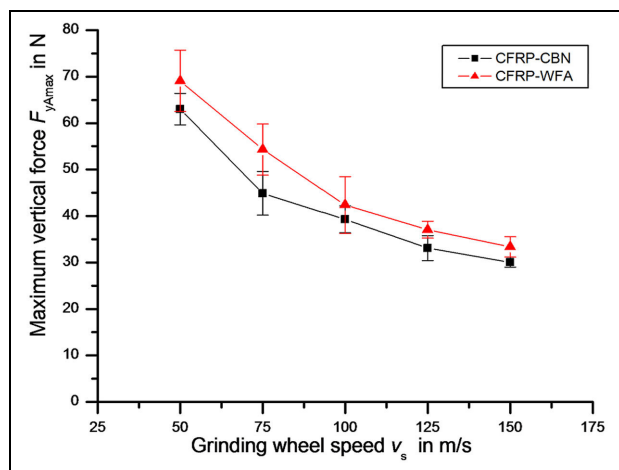
the observed force components decreased with increasing grinding wheel speed. At each test point, lower maximum tangential forces F_{tsmax} were measured for the CFRP-CBN grinding wheel (Modification 1) than for the CFRP-WFA grinding wheel (Modification 2). This indicates that the CFRP-WFA grinding wheel has an higher effective grinding wheel hardness compared to the CFRP-CBN grinding wheel.

The reduction of the maximum tangential forces with a grinding wheel speed between 50 and 150 m/s is about 30% for both modifications. The high grinding wheel speed results in an equivalent decline of the chip thickness and thus the loads on the grain.[3]

Maximum vertical force F_{yAmax} on the workrest blade

Similar to the results of the maximum tangential force F_{tsmax}, the maximum vertical forces F_{yAmax} decreased significantly with an increasing grinding wheel speed (Figure 9). For the CFRP-CBN grinding wheel as well as for the CFRP-WFA grinding wheel, the maximum vertical forces for the full range of tested grinding wheel speeds reduced by more than 50%.

With increasing grinding wheel speed and therefore decreasing maximum vertical forces F_{yAmax}, both the

Figure 9. Maximum vertical force F_{yAmax} as a function of the grinding wheel speed v_s.
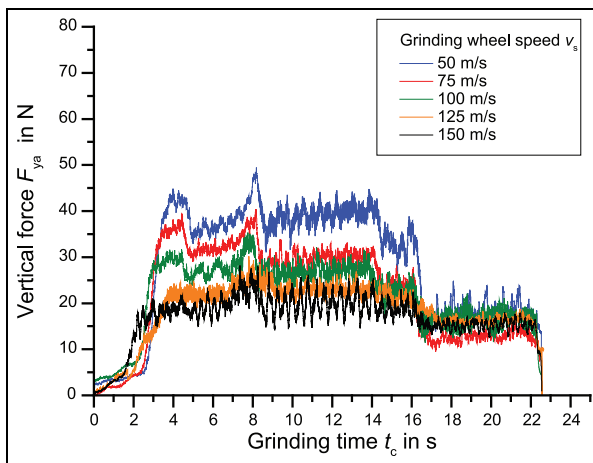
normal and the tangential components of the force F_A were reduced.

Since the equivalent chip thickness is being reduced by increasing grinding wheel speed, the grain wear is reduced and the surface quality can be enhanced.[13]
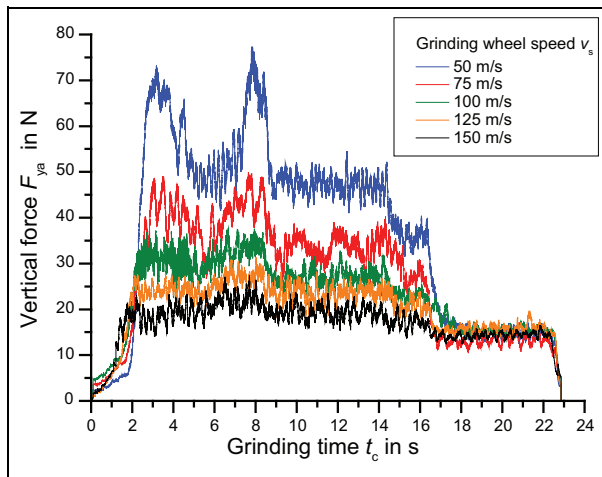
Figure 10. Force progression of the vertical force F_{yA} for CFRP-WFA.

Figure 11. Force progression of the vertical force F_{yA} for CFRP-CBN.

Force progression

Detailed statements about the effects of forces can be achieved by the force progression of the grinding process. The average force progressions are calculated from four individual progressions.

In Figures 10 and 11, the force progressions of the vertical force F_{yA} are illustrated for the CFRP-WFA grinding wheel and CFRP-CBN grinding wheel, respectively.

The course of each graph shows several plateaus indicating the different process steps. For most process steps, the plateaus remain constant with little deviations.

However, this does not apply to the rough machining step. This is reasoned by the fact that the grinding wheel is in contact with the workpiece initially on the large diameter, then on the small diameter and, finally, on the bearing track. The grinding wheel only engages

over the entire length of the shaft component during the first semi-finishing stage. The reason is that in order to ensure process stability, the tool has a larger profile section than the difference between the large and small shaft diameter on the test workpiece (about $200 \, \mu m$).

The vertical forces F_{yA} are significantly lower for the complete grinding process at a grinding wheel speed of $150 \, m/s$ compared to the tests at $50 \, m/s$. Furthermore, it is apparent that the force differences between the process steps at $150 \, m/s$ can hardly be perceived. This constitutes an approximately uniform stress load. It is significant that the peak load at the beginning is less than the described maximum force at the end of rough machining. Furthermore, the dispersion of the maximum vertical force decreases with the increasing grinding wheel speed.

A uniform force profile with reduced dispersion lowers the risk of dynamic instability and decreases the formation of roundness errors and chatter marks. With regard to grain wear, equal loads should have a positive impact and reduce the risk of grain breaking.

Using the CFRP-CBN grinding wheel, fluctuations of the forces were detected at $v_s = 150 \, m/s$. The reasons were slight differences in the workpiece edge zone by geometrical and material-specific tolerances of the test pieces and, therefore, slight changes in the grinding conditions. Another reason may be deteriorated contact conditions between the workpiece and the regulating wheel, due to slightly different coefficient of friction μ_r.

It is remarkable that for a grinding wheel speed of $150 \, m/s$, the measured vertical forces are approximately equal for both grinding wheel modifications. At lower grinding wheel speeds, however, significantly lower forces for the CFRP-CBN grinding wheel are evident. This leads to the conclusion that even at high grinding wheel speeds, conventional abrasives have a good cutting ability.

Surface quality roughness R_a and R_z

In Figures 12 and 13, the evaluation of the arithmetic mean roughness R_a and the averaged roughness height R_z are illustrated, respectively. With the increase of the grinding wheel speed, the arithmetical mean roughness R_a using both grinding wheel modifications can be regarded as constant. The predetermined quality restrictions of $R_z < 3 \, \mu m$ and $R_a < 0.5 \, \mu m$ can be adhered to all test points.

It appears, however, that with an increase of the grinding wheel speed, the scattering of the roughness parameter rises. Several reasons are possible: process-induced vibrations can be triggered by a dynamic imbalance in the grinding wheel, higher temperatures have an impact on the contact zone or an insufficient coolant supply has increased the dispersion of the roughness.
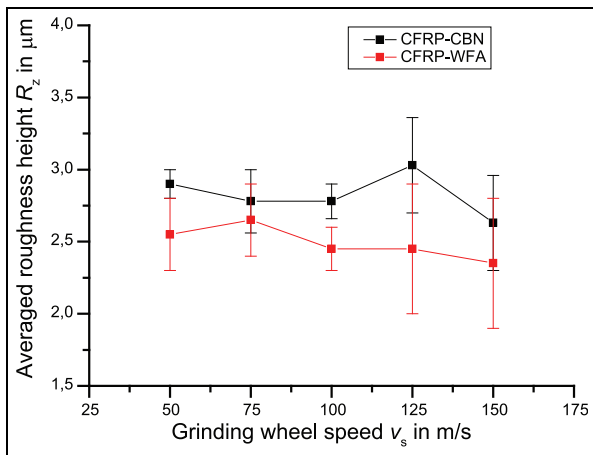
Figure 12. Averaged roughness height R_z as a function of the grinding wheel speed v_s.
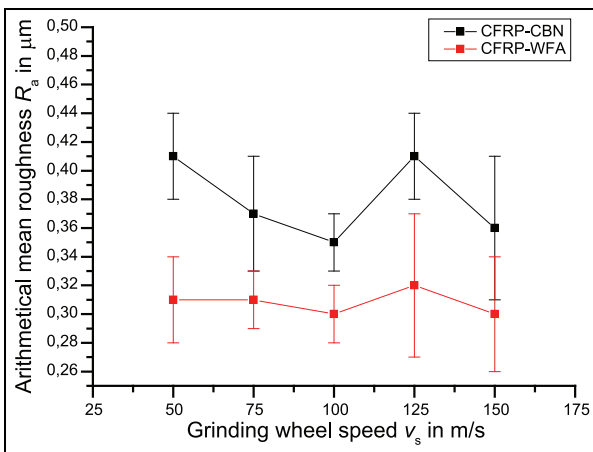
Figure 13. Arithmetical mean roughness R_a as a function of the grinding wheel speed v_s.

This analysis shows furthermore that the grinding wheel specification in the form of grain type, grain size and concentration essentially determines the surface quality. An improvement in the surface quality is barely visible through the increase in the grinding wheel speed.

This result proves that a high degree of surface quality using high-speed plunge-cut centreless grinding can also be produced applying conventional abrasives. These results can be integrated into an intelligent system for the computer-based selection of grinding wheels regarding the grain as well as the body structure.[14]

Summary

To realise the high grinding wheel speed, new grinding wheels have been developed, which have a CFRP grinding wheel base body with only one-quarter of the mass of a steel base body. The technical operational capability for grinding wheel speeds up to 150 m/s could be proven with these experiments through the use of the test machine MIKROSA KRONOS S 250. In order to measure the maximum vertical force F_{yAmax} on the workrest blade, a new workrest blade with integrated force measuring sensors has been designed, and its applicability for these test parameters has also been substantiated.

In this study, a reduction of the maximum tangential force F_{tsmax} and the maximum vertical force F_{yAmax} of more than 30% and 50% were measured for a WFA grain and a CBN grain by increasing the grinding wheel speed from 50 m/s up to 150 m/s, respectively.

A high grinding wheel speed (>120 m/s) generates uniform force progression, which has a positive impact on the grain wear and lowers the risk of grain breakout. As a result, conditioning cycles can be extended and non-productive times reduced.

In addition, this study shows that conventional abrasives, such as WFA grain, can be used in high-speed grinding. The tangential and vertical forces (F_{tS} and F_{yA}) decrease by the same amounts as a CBN grain and approach by rising grinding wheel speeds. This illustrates enormous potential in saving tooling costs, since conventional abrasives are multiple times cheaper than super abrasives.

The analysis of the surface quality showed that with the increase in the grinding wheel speed, the quality parameters R_z and R_a remain nearly constant. In addition, at each test point, the CFRP-WFA grinding wheel produces a lower roughness parameter on the workpiece compared to the CFRP-CBN grinding wheel, which further confirms the potential use of conventional abrasives.

References

1. Oliveira JFG, Silva EJ, Guo C, et al. Industrial challenges in grinding. *CIRP Ann: Manuf Techn* 2009; 58(2): 663–680.
2. Hashimotoa F, Gallego I, Oliveira JFG, et al. Advances in centerless grinding technology. *CIRP Ann: Manuf Techn* 2012; 61(2): 747–770.

3. Klocke F and König W. *Fertigungsverfahren 2: Schleifen, Honen, Läppen*. Berlin, Heidelberg: Springer-Verlag, 2005.

4. Li H and Shin YC. A time domain dynamic simulation model for stability prediction of infeed centerless grinding processes. *J Manuf Sci Eng* 2007; 129(3): 539–550.

5. Harrison AJL and Pearce TRA. Prediction of lobe growth and decay in centreless grinding based on geometric considerations. *Proc IMechE, Part B: J Engineering Manufacture* 2002; 216(9): 1201–1216.

6. Jameson JR, Farris TN and Chandrasekar S. Equilibrium and compatibility simulation of plunge centreless grinding. *Proc IMechE, Part B: J Engineering Manufacture* 2008; 222(7): 747–757.

7. Pearce TRA and Stone BJ. Unstable vibration in centreless grinding: part 1. Geometric instability or chatter? *Proc IMechE, Part B: J Engineering Manufacture* 2011; 225(B8): 1227–1243.

8. Tawakoli T, Reinecke H and Vesali A. An experimental study on the dynamic behavior of grinding wheels in high efficiency deep grinding. *Procedia CIRP* 2012; 1: 382–387.

9. Meyer B. *Prozesskräfte und Werkstückgeschwindigkeiten beim Spitzenlosschleifen*. Aachen: Apprimus Verlag, 2010.

10. Hannig, S. *Analyse, Modellierung und Simulation des dynamischen Verhaltens beim spitzenlosen Einstechschleifen*. Aachen: Shaker, 2008, p.154.

11. Rowe WB. Rounding and stability in centreless grinding. *Int J Mach Tools Manuf* 2014; 82–83: 1–10.

12. Barrenetxea D, Alvarez J, Marquinez JI, et al. Stability analysis and optimization algorithms for the set-up of infeed centerless grinding. *Int J Mach Tools Manuf* 2014; 84: 17–32.

13. Bierlich, R. *Technologische Vorraussetzung zum Aufbau eines adaptiven Regelungssystems beim Außenrundeinstechschleifen*. Aachen: na, 1976, p.145.

14. Li Y, Mills B and Rowe WB. An intelligent system for selection of grinding wheels. *Proc IMechE Part B, J Engineering Manufacture* 1997; 211(8): 635–641.

Appendix I

Notation

a_e	width of cut (μm)
F_A	resultant force, workrest blade (N)
F_{gw}	weight force of the workpiece (N)
F_{nA}	normal force, workrest blade (N)
F_{nR}	normal force, regulation wheel (N)
F_{nS}	normal force, grinding wheel (N)
F_{tA}	tangential force, workrest blade (N)
F_{tR}	tangential force, regulation wheel (N)
F_{tS}	tangential force, grinding wheel (N)
F_{tsmax}	maximum tangential force, grinding wheel (N)
F_{xA}	horizontal force, workrest blade (N)
F_{yA}	vertical force, workrest blade (N)
F_{yAmax}	maximum vertical force, workrest blade (N)
P_c	cutting power (W)
P_l	idle load power (W)
P_t	total power (W)
R_a	arithmetical mean roughness (μm)
R_z	averaged roughness height (μm)
t_c	grinding time (s)
$v_{r_{1,2}}$	radial feed speed (mm/s)
v_s	grinding wheel speed (m/s)
v_w	workpiece peripheral speed (m/s)
β	workrest blade angle
μ_r	friction coefficient of regulation wheel